Effects of Ion Bombardment on the Chemical Reactivity of GaAs(100): Variation of Bombarding Ion Mass

J. M. Epp,† J. G. Dillard,*,† A. Siochi,‡ R. Zallen,‡ S. Sen,§ and L. C. Burton§

Chemistry Department, Physics Department, and Electrical Engineering Department, Virginia Polytechnic Institute and State University, Blacksburg, Virginia 24061-0212

Received October 5, 1989

The effect of the mass of the bombarding ion on the chemical reactivity of ion-bombarded GaAs(100) was investigated by X-ray photoelectron spectroscopy. Chemically cleaned (1:1 HCl(conc)/H_2O) GaAs was ion bombarded with 3-keV $^3He^+$, Ne^+, Ar^+, and Xe^+ at a constant fluence (10^{17} ions/cm^2) and subsequently exposed to O_2 in the range 10^7–10^{11} langmuirs and H_2O at 10^{13} langmuirs. Ion-bombarded GaAs exposed to O_2 yields Ga_2O_3, As_2O_3, and As_2O_5, with Ga_2O_3 being the major component. Exposure of ion-bombarded GaAs to H_2O yields GaO(OH) and $Ga(OH)_3$. Ion-bombarded GaAs shows an increased chemical reactivity compared to that of chemically cleaned GaAs, and the enhancement in reactivity was shown to be directly related to the mass of the bombarding ion. Upon exposure to either O_2 or H_2O, GaAs ion bombarded with 3-keV Xe^+ ions exhibited the greatest chemical reactivity, which suggests that defects caused by ion bombardment are concentrated at the surface and play a role in the enhanced chemical reactivity. The damage caused by ion bombardment was also investigated by optical reflectivity in the visible and near-ultraviolet region, by Raman spectroscopy and by current-voltage and capacitance-voltage measurements. Ion bombardment forms a structurally damaged near-surface layer. The depth of damage is inversely related to the mass of the bombarding ion. X-ray photoelectron spectroscopy detected crystal damage in the form of As depletion that extends through the first 60 Å of the GaAs crystal in all cases, with the magnitude of As depletion increasing with increasing ion-bombardment mass. Bombardment of GaAs with 3-keV Xe^+ ions produces a greater defect density at the surface, leading to increased chemical reactivity.

Introduction

Ion bombardment of GaAs affects the surface reactivity of GaAs, and the magnitude of the effect is related to the ion-bombardment energy. Changes in the chemical reactivity of GaAs have been linked to defects caused by ion bombardment.[1-4] It was previously shown that Ar^+-ion-bombarded GaAs (0.5–3 keV) showed an increased chemical reactivity compared to that of chemically cleaned,[4] cleaved,[1] or sputter/annealed GaAs[5] when exposed to O_2 (10^7–10^{13} langmuirs) and H_2O (10^9–10^{12} langmuirs) (1 langmuir = 1.3×10^{-4} Pa·s). For both O_2 and H_2O, the reactivity increased with increasing Ar^+-ion-bombardment energy up to 2 keV. The increase in reactivity with increasing ion-bombardment energy supports the conclusions of others[1,2,6,7] that the reaction of gases takes place on the GaAs surface at defect sites formed by ion bombardment. Comparison of oxidation results for ion-bombarded material with those for IHT[8] (simultaneously ion bombarded and heated) prepared material substantiated this result.[4]

McGuire[9] and Holloway and Battacharya[10,11] noted that the surface composition is dependent on both the energy and mass of the incident bombarding ion. The mass (M_1) of the primary bombarding ion determines the maximum amount of energy that can be transferred to an atom of mass M_2 in the target at a given energy E_0[12]:

$$T_{max} = \gamma E_0 = [(4M_1M_2)/(M_1 + M_2)^2]*E_0 \quad (1)$$

The penetration depth of the primary ion into the target is also determined by size. Lighter ions are expected to transfer less energy to the substrate upon collision but can penetrate deeper into the target due to their size. Because a lighter ion loses less of its initial energy upon collision with the surface atoms, it is able to penetrate deeper into the surface because it is not stopped as quickly as is a heavier ion (nuclear stopping power).[13] The initial transfer of energy and penetration depth are responsible for setting a collision cascade into motion that in turn determines how much damage is done and how deep the damage layer is.

The change in surface chemical composition as a function of ion energy for a primary ion of fixed mass was previously studied,[4] and it was shown that damage induced on the surface affected the chemical reactivity of the material. Additionally, the chemical reactivity of a material could be affected to different degrees depending on the amount and depth of surface damage caused by bombarding ions of different masses. It is the purpose of this work to study the effect of the incident bombarding ion mass (fixed energy) on the surface composition and on the chemical reactivity of GaAs with O_2 and H_2O.

Ion bombardment can cause damage deep into a material (>100 Å).[8,14-18] X-ray photoelectron spectroscopy

† Chemistry Department.
‡ Physics Department.
§ Electrical Engineering Department.

(1) Chye, P. W.; Su, C. Y.; Lindau, I.; Skeath, P.; Spicer, W. E. *J. Vac. Sci. Technol.* **1979**, *16*, 1191.
(2) Mark, P.; Creighton, W. F. *Thin Solid Films* **1979**, *56*, 19.
(3) Mark, P.; So, E.; Bonn, M. *J. Vac. Sci. Technol.* **1977**, *14*, 865.
(4) Epp, J. M.; Dillard, J. G. *Chem. Mater.* **1989**, *1*, 325.
(5) Webb, C.; Lichtensteiger, M. *J. Vac. Sci. Technol.* **1982**, *21*, 659.
(6) Goddard III, W. A.; Barton, J. J.; Redondo, A.; McGill, T. C. *J. Vac. Sci. Technol.* **1978**, *15*, 1274.
(7) Brundle, C. R.; Seybold, D. *J. Vac. Sci. Technol.* **1979**, *16*, 1186.
(8) Oelhafen, P.; Freeouf, J. L.; Pettit, G. D.; Woodall, J. M. *J. Vac. Sci. Technol. B* **1983**, *1*, 787.
(9) McGuire, G. E. *Surf. Sci.* **1978**, *76*, 130.
(10) Holloway, P. H.; Battacharya, R. S. *J. Vac. Sci. Technol.* **1982**, *20*, 444.
(11) Battacharya, R. S.; Holloway, P. H. *Appl. Phys. Lett.* **1981**, *38*, 85.
(12) Sigmund, P. In *Sputtering by Particle Bombardment I: Physical Sputtering of Single-Element Solids*; Berisch, R., Ed.; Springer-Verlag: Berlin, 1981; pp 10–70.
(13) Benninghoven, A.; Rüdenauer, F. G.; Werener, H. W. *Secondary Ion Mass Spectrometry: Basic Concepts, Instrumental Aspects, Application, and Trends*; Wiley: New York, 1987; pp 26, 43, and 1109.
(14) Pang, S. W. *Solid State Technol.* **1984**, *27*, 249.
(15) Pang, S. W.; Geis, M. W.; Efremow, N. N.; Lincoln, G. A. *J. Vac. Sci. Technol. B* **1985**, *3*, 398.
(16) Singer, I. L.; Murday, J. S.; Comas, J. *J. Vac. Sci. Technol.* **1981**, *18*, 161.

0897-4756/90/2802-0173$02.50/0 © 1990 American Chemical Society

(XPS) is able to probe only about 60 Å into the surface, and the only evidence for ion bombardment damage is the change in the Ga/As ratio and the presence of implanted ions. To probe the depth of damage effects and perhaps obtain some correlation between ion bombardment and reactivity, electrical studies (*I–V* and *C–V* characteristics) and optical studies (Raman and optical reflectivity) of GaAs were also conducted. These studies involved the evaluation of ion-bombarded and nonbombarded (crystalline) GaAs(100).

Experimental Section

Materials. In this study n-type GaAs(100) with a Si doping density $\leq 5 \times 10^{17}$ cm^{-3} was used. All specimens were cleaned in 1:1 HCl(conc)/H_2O (vol/vol) at room temperature for 10 min to remove surface oxides and were subsequently rinsed in deionized water. Samples so treated are referred to as chemically cleaned GaAs. The samples were transferred in air to the XPS chamber for ion bombardment and reactant gas exposure.

Ion Bombardment. Ion bombardment was carried out in a Perkin-Elmer Model 5300 XPS system equipped with a 04-300 differentially pumped ion gun, mounted at 45° with respect to a line perpendicular to the specimen surface. $^3He^+$ (Isotec Inc., 99.9%), $^{20}Ne^+$ (Isotec, 99.95%), $^{40}Ar^+$ (Union Carbide, Research Grade), and Xe^+ (Airco, 99.9995%, natural isotopic abundance) ion bombardments were carried out at 3000 eV using a 1-cm^2 rastered beam with currents in the range 20–30 μA. The time of bombardment was adjusted to give fluences in the range $(7.5 \pm 1.5) \times 10^{17}$ ions·cm^{-2}. The samples were oriented such that ion bombardment was in the (111) direction. Chamber pressure during ion bombardment was generally about 10^{-5} Pa.

Gas Exposures. Following ion bombardment, the sample was transferred under vacuum into a stainless steel ultrahigh-vacuum reaction chamber attached to the XPS system where exposures to O_2 or to H_2O vapor were carried out. Oxygen purchased from Airco (99.993%) was passed through an Alltech gas purifier that contained indicating Drierite and 5-Å molecular sieves before being introduced into the reaction chamber. Deionized H_2O was boiled, cooled by bubbling N_2 through the liquid, placed in a stainless steel Nupro sample cylinder, and connected to the reaction chamber. Further purification of H_2O occurred by a freeze/thaw cycle under vacuum. Oxygen exposures ranged from 10^7 to 10^{11} langmuirs, and H_2O exposure was 10^{13} langmuirs. All gas exposures were done at room temperature. Care was taken to avoid exposure to exicted oxygen.[4]

Surface Analysis. The surfaces were analyzed by XPS using Mg Kα radiation ($h\nu$ = 1253.6 eV) as the excitation source and with a chamber pressure of less than 4×10^{-6} Pa. Spectra were obtained immediately following ion bombardment and also immediately following reactant gas exposure for the Ga 3d, As 3d, and O 1s core levels at various takeoff angles (TOA). The takeoff angle is measured as the angle between a line in the sample surface and a line to the entrance of the photoelectron analyzer. The photopeaks were analyzed by subtracting the X-ray source line width, smoothing, and curve-resolving using Gaussian peak shapes. Software routines available with the PHI 5300 system were used. The atomic concentrations were evaluated from photopeak areas by using the appropriate sensitivity factors.

About 95% of the observed photoelectron signal comes from a layer $3\lambda \sin \theta$ thick, where θ is the takeoff angle and λ is the mean free path of the photoelectron.[19] For the Ga 3d and As 3d core levels, λ is approximately 22 Å; therefore, the analysis depths for the Ga 3d and As 3d photoelectrons at 15 and 90° TOAs are approximately 17 and 66 Å, respectively.[4] For the Xe $3d_{5/2}$ and Ne 1s core levels λ is approximately 9 and 12 Å, respectively; therefore, the analysis depths vary between 7 and 28 Å for the Xe $3d_{5/2}$ level and 10 and 37 Å for the Ne 1s level when the TOA is varied between 15 and 90°, respectively.

(17) Singer, I. L.; Murday, J. S.; Cooper, L. R. *Surf. Sci.* **1981**, *108*, 7.
(18) Kawabe, M.; Kanzaki, N.; Masuda, K.; Namba, S. *Appl. Opt.* **1978**, *17*, 2556.
(19) Briggs, D. In *Practical Surface Analysis by Auger and X-ray Photoelectron Spectroscopy*; Briggs, D., Seah, M. P., Eds.; Wiley: New York, 1983; p 362.

Table I. Ga/As Atomic Ratios for Chemically Cleaned and Ion-Bombarded GaAs (3 keV, 10^{17} ions/cm^2)

	Ga/As[a]	
	TOA = 15°	TOA = 90°
chemically cleaned	0.78 ± 0.05	0.89 ± 0.05
Xe^+	1.73 ± 0.07	1.73 ± 0.03
Ar^+	1.50 ± 0.05	1.53 ± 0.05
Ne^+	1.32 ± 0.05	1.36 ± 0.04
$^3He^+$	1.16 ± 0.08	1.22 ± 0.05

[a] Ga/As ratio determined from (peak area)/σ, where peak area is Ga 3d or As 3d photopeak area and σ is the appropriate sensitivity factor.

Spectra for model compounds Ga_2O_3 (Alfa, 99.99%), As_2O_3 (Aldrich, 99.999%), As_2O_5 (Fisher, 99.2%), and GaO(OH) (synthesized) were used for the determination of binding energies, full widths at half-maxima (fwhm), and atomic ratios.[4] GaO(OH) was prepared by using the procedure described previously.[4]

Electrical Measurements. For electrical characterization, Schottky diodes were formed on GaAs. Ohmic metal, AuGe (88%–12%), was deposited on samples, followed by Ni deposition and annealing at 440 °C for 2 min under forming gas (90% N_2 + 10% H_2). The samples with ohmic contacts were chemically cleaned and then ion bombarded. The control sample (no ion bombardment) was also chemically cleaned. Schottky metal (aluminum) was then deposited on the ion bombarded and control samples. Current–voltage and capacitance–voltage measurements on the samples were done at room temperature (290 K).

Optical Measurements. Raman spectra were measured in a backscattering geometry by using the 4579-Å (2.71 eV) line of an Ar-ion laser as the excitation source.[20] Optical reflectivity spectra were measured at near-normal incidence in the visible and near-ultraviolet region (photon energy ranging from 1.6 to 5.6 eV). Raman intensity measurements were made using crystalline GaAs as a reference standard. All of the optical experiments were carried out at room temperature.

Results and Discussion

Ion-Bombardment Effects on GaAs Surface Composition. a. Surface Stoichiometry. Chemically cleaned GaAs was ion bombarded with $^3He^+$, $^{20}Ne^+$, $^{40}Ar^+$, and Xe^+ at 3 keV (10^{17} ions/cm^2) to determine what effect the incident bombarding ion mass would have on the surface composition and reactivity. The relative amounts of Ga(GaAs) and As(GaAs) on the surface as determined from XPS measurements taken at 15 and 90° TOAs following chemical cleaning and ion bombardment with different mass ions are summarized in Table I. Ion bombardment of GaAs removes residual oxygen from the chemically cleaned surface, which contained $\approx$36 ± 9 at. % (15° TOA) and $\approx$16 ± 7 at. % (90° TOA) oxygen.[4] For surfaces bombarded with different ions at 3 keV, no residual oxygen (<2 at. %) was detected, and therefore, only the Ga/As atomic ratio is reported. Arsenic is preferentially sputtered from the GaAs surface in all cases as indicated by the Ga/As atomic ratios, which are all greater than 1. The extent of As depletion is greater following bombardment with the heavier ions.

Figure 1 shows the Ga/As atomic ratios following chemical cleaning and ion bombardment as a function of TOA. The Ga/As atomic ratio at different TOAs can be used to evaluate the depth of damage (detected as As depletion) caused by the different bombarding ions. For each ion, the extent of As depletion is fairly uniform over the depth examined ($\approx$60 Å). The Ga/As ratios for the respective ions are equivalent within the experimental error. The values given for $^3He^+$ in Figure 1 also indicate the same trend. However, the data for Ne^+ indicate a

(20) Holtz, M.; Zallen, R.; Brafman, O.; Matteson, S. *Phys. Rev. B* **1988**, *37*, 4609.

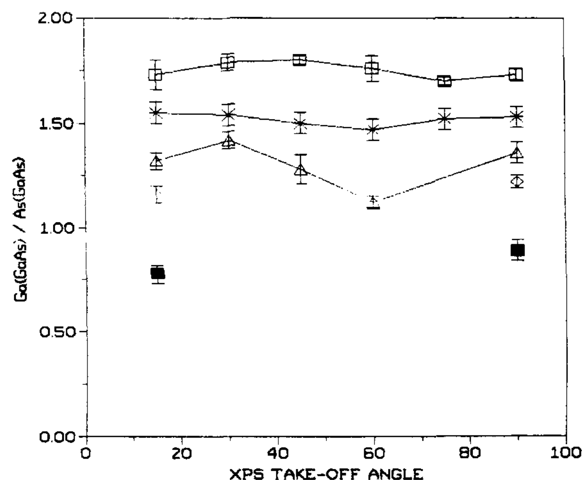

Figure 1. Ga/As atomic ratios following chemical cleaning (■) and 3-keV Xe^+ (□), Ar^+ (✱), Ne^+ (△), and $^3He^+$ (◇) ion bombardment as a function of XPS takeoff angle.

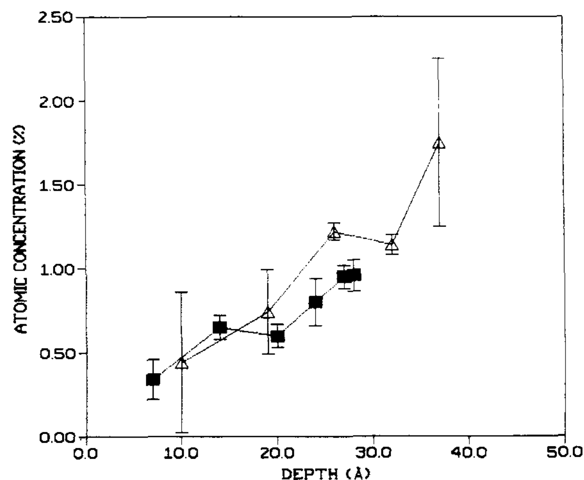

Figure 2. Atomic concentrations of Xe (■) and Ne (△) found in GaAs following 3-keV ion bombardment.

Table II. Energy Differences ΔE between As 3d and Ga 3d Photopeaks for Various Bonding States

condition	ΔE, eV
GaAs (cleaved)[a]	22.0 ± 0.2
Ga^0 and As^0[a]	23.4 ± 0.2
Ga^0 and As(GaAs)[a]	22.8 ± 0.2
As^0 and Ga(GaAs)[a]	22.6 ± 0.2
chemically cleaned[b]	21.9 ± 0.2
ion bombarded[b]	22.0 ± 0.2

[a] From ref 23, 27, and 33. [b] This work.

slight nonuniformity in As depletion (at 60° TOA) with depth, although the ratio is just outside the experiment error of the measurement. Even though As depletion of an ion-bombarded surface is unanimously reported in the literature, the uniformity in As depletion of the damaged surface layer is not agreed upon.[21,22]

b. Chemical State of Ga and As in the Damaged Layer. The chemical state of Ga and As in the ion-bombarded material can be obtained from the XPS data. To inquire how As depletion is accommodated in ion-bombarded GaAs, the energy differences between the As 3d and Ga 3d photopeaks[21] are considered in Table II. Elemental Ga (BE = 18.2 eV)[23] and As (BE = 41.7 eV)[23] exhibit different binding energies than those for Ga or As combined in GaAs. If ion bombardment resulted in the formation of either elemental Ga combined with As(GaAs) or elemental As combined with Ga(GaAs), then the energy differences between the As 3d and Ga 3d photopeaks would reflect the presence of either As^0 or Ga^0 combined with GaAs. The binding energy differences between the As 3d and Ga 3d photopeaks obtained in this study do not indicate a change in the chemical state of either As or Ga as a result of ion bombardment. The energy difference, ΔE(As 3d–Ga 3d), for ion-bombarded GaAs, regardless of the ion-bombardment mass, is equivalent to that obtained for chemically cleaned GaAs and the literature values for cleaved GaAs (see Table II). Thus, it can be concluded that the resulting ion-bombarded surface is not a combination of both Ga and As in elemental form.

In this study no change in the binding energy for either the Ga 3d or As 3d photopeaks upon ion bombardment was noted; however, there was a slight broadening in the Ga 3d photopeak following ion bombardment. The fwhm of chemically cleaned GaAs was 1.0 ± 0.1 eV, and the fwhm of ion bombarded GaAs was consistently wider, 1.2 ± 0.1 eV. Since the peak broadening was small, it was difficult to determine whether the broadening was due to elemental Ga formation. The slight peak broadening could be caused by increased disorder in the surface as a result of ion-bombardment damage such that stronger Ga–Ga bonds and weaker Ga–As bonds are present in an ion-bombarded surface.[16,24] The As deficiency created by ion bombardment suggests that a substantial number of Ga atoms in the surface region should have other Ga atoms as nearest neighbors. The XPS data do not permit one to establish whether the Ga atoms are unbonded, producing dangling bonds, or whether As deficiencies are replaced by Ga–Ga "wrong" bonds.[25] Bonds between like atoms destroy the chemical order and could account for the broadening observed in the Ga 3d photopeak for ion-bombarded GaAs. It is also possible that broadening could be produced by Ga atoms having other Ga atoms as near neighbors without being bonded to them, since the lack of As atoms next to Ga atoms would change the chemical (electrostatic) environment around Ga atoms compared to the original GaAs environment. The binding energy of Ga atoms with other Ga atoms as nearest neighbors, whether bound or not, could be reduced; Ga metal has a lower binding energy than Ga of GaAs. No changes in the shape or width of the As 3d photopeak were observed following ion bombardment.

c. Ion Implantation. Due to the relatively large photoionization cross sections for the Xe $3d_{5/2}$ and Ne 1s levels,[26] it was possible to detect these atoms in GaAs following ion bombardment. The atomic concentrations for 3-keV Ne^+ and Xe^+ implanted in GaAs as a function of depth (determined from different TOAs) are shown in Figure 2. The bombarding ions become implanted in GaAs at least as deep as can be detected by XPS (limited by the mean free path of electrons from either Xe or Ne). The amount of Ne implanted is greater than that of Xe at ≈28 Å, and it becomes even greater (1.5 at. %) for Ne at ≈37 Å. This buildup could be controlled by the sputter rate and the penetration depth. The sputter yield for Xe^+

(21) Wang, Y.-X.; Holloway, P. H. *J. Vac. Sci. Technol. B.* **1984**, *2*, 613.
(22) Bussing, T. D.; Holloway, P. H.; Wang, Y. X.; Moulder, J. F.; Hammond, J. S. *J. Vac. Sci. Technol. B* **1988**, *6*, 1514.
(23) Mizokawa, Y.; Iwasaki, H.; Nishitani, R.; Nakamura, S. *J. Electron Spectrosc. Relat. Phenom.* **1978**, *14*, 129.
(24) Su, C. Y.; Lindau, I.; Chye, P. W.; Skeath, P.; Spicer, W. E. *Phys. Rev. B.* **1982**, *25*, 4045.
(25) Shevchik, N. J.; Tejeda, J.; Cardona, M. *Phys. Rev. B* **1974**, *9*, 2627.
(26) Scofield, J. H. *J. Electron Spectros. Relat. Phenom.* **1976**, *8*, 129.

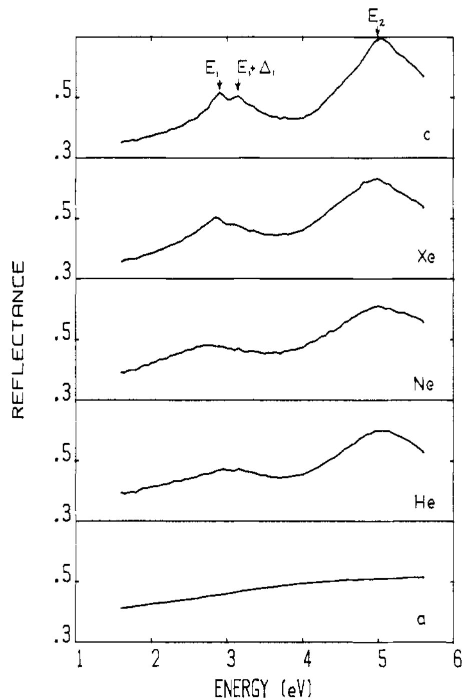

Figure 3. Optical reflectivity spectra obtianed for crystalline, 3-keV Xe^+, Ne^+, $^3He^+$, ion-bombarded, and amorphous GaAs (top to bottom, respectively).

→ GaAs would be expected to be greater than that for Ne^+ → GaAs, and Ne^+ is expected to have a deeper penetration into GaAs.[13] Thus a buildup of Ne in GaAs would be expected. The binding energies for Xe and Ne implanted into GaAs are 669.7 ± 0.2 eV and 863.6 ± 0.2 eV, respectively. These binding energies are the same as those obtained for the Ne and Xe implanted in other materials such as C, Fe, and Cu[27,28] and indicate that they are interstitial atoms and do not interact chemically with the GaAs lattice.

Depth of Damaged Layer. Information about the structural disorder in ion-bombarded GaAs was obtained from the electrical and optical measurements. Crystalline GaAs exhibits a characteristic reflectivity spectrum in the photon energy range 1.5–5.6 eV, and any decrease in the crystallinity and increase in disorder alters the appearance of the spectrum.[20,29–32] In this photon energy range the optical penetration depth is the order of 100 Å,[20,31,32] and thus the bombardment-induced damage to the crystal structure can be probed to a depth that is greater than that probed by XPS.

Figure 3 shows a series of visible–ultraviolet reflectivity spectra acquired for GaAs bombarded with 3-keV Xe^+, Ne^+, and $^3He^+$ ions. Also shown for comparison are the spectra of crystalline and completely amorphous GaAs.[32] The spectra reflect the direct (k-vector conserved) interband electronic transitions. The three main peaks in the

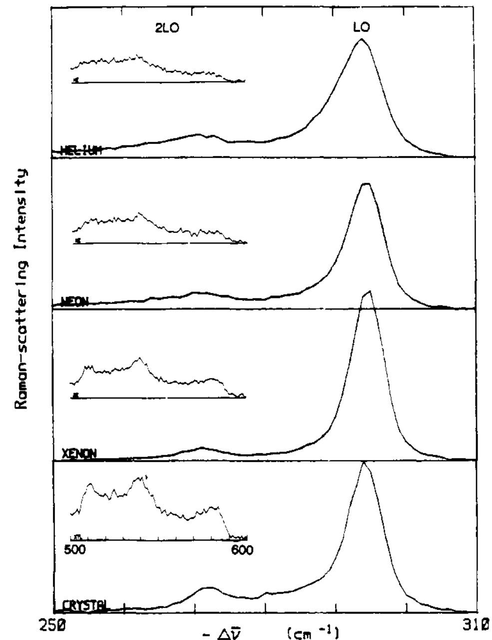

Figure 4. Raman spectra obtained for crystalline, 3-keV Xe^+-, Ne^+-, and $^3He^+$-ion-bombarded GaAs (bottom to top, respectively).

spectrum for crystalline GaAs are conventionally denoted as E_1 (2.9 eV), $E_1 + \Delta_1$ (3.1 eV, which is the spin–orbit splite component of E_1), and E_2 (5.0 eV).[31] It is important to note the changes in shape and intensity of the three main peaks when comparing crystalline GaAs to ion-bombarded GaAs.

Ion bombardment destroys the crystalline order in the near-surface region. The damage is revealed by the decrease in intensity of the E_2 peak, the broadening of both the E_1 and E_2 peaks, and the loss of the E_1, $E_1 + \Delta_1$ doublet structure. These changes indicate a decrease in structural order near the surface. Since the three sharp peaks associated with crystallinity will be present if the damage layer is thinner than the optical penetration depth, these results provide information about the damage-layer thickness. The reflectivity spectrum loses progressively more of its crystalline characteristics with decreasing ion mass, showing that the depth of damage is inversely related to the ion mass. A detailed optical study of Ar^+-ion-bombarded samples,[30] done as a function of chemical-etch removal of surface layers, shows a nearly linear falloff in damage with depth, with the half-depth being about 250 Å in this case. Unlike the case of high-energy ion implantation, which creates a mixed amorphous/microcrystalline damage layer,[20] the damage layer produced by low-energy ion bombardment (as studied here) is more complex and appears to consist of a highly disturbed crystalline layer characterized by a high density of point defects.[30]

The Raman spectra observed for crystalline GaAs and for GaAs ion bombarded with $^3He^+$, Ne^+, and Xe^+ at 3 keV are shown in Figure 4. An estimate of the depth of damage caused by bombardment (constant energy and fluence) can be obtained by examining these spectra. At the laser photon energy of 2.71 eV, the absorption coefficient α is larger for amorphous GaAs than for crystalline GaAs. The laser beam probing depth $1/(2\alpha)$ is about 250 Å for crystalline GaAs and 100 Å for amorphous GaAs.[29,32] For these ion-bombarded samples, the probing depth is expected to be closer to the crystalline value.[30] The sharp, intense peak in the Raman spectra at 292 cm^{-1} corresponds to the first-order longitudinal-optical (LO) Raman line in crystalline GaAs. The peaks in the region 500–580 cm^{-1} cor-

(27) Wagner, C. D. In *Practical Surface Analysis by Auger and X-ray Photoelectron Spectroscopy*; Briggs, D., Seah, M. P., Eds.; Wiley: New York, 1983; Appendix 4.
(28) Wagner, C. D.; Riggs, W. M.; Davis, L. E.; Moulder, J. F. *Handbook of X-Ray Photoelectron Spectroscopy*; Muilenberg, G. E., Ed.; Perkin-Elmer: Eden Prairie, MN, 1979.
(29) Aspnes, D. E.; Kelso, S. M.; Olson, C. G.; Lynch, D. W. *Phys. Rev. Lett* **1982**, *48*, 1863.
(30) Feng, G. F.; Zallen, R.; Epp, J. M.; Dillard, J. G., to be published.
(31) Feng, G. F.; Holtz, M.; Zallen, R.; Epp, J. M.; Dillard, J. G.; Cole, E.; Johnson, P.; Sen, S.; Burton, L. C. *Mater. Res. Soc. Sym. Proc.* **1987**, *93*, 381.
(32) Feng, G.; Zallen, R. *Phys. Rev. B* **1989**, *40*, 1064.
(33) Pianetta, P.; Lindau, I.; Garner, C. M.; Spicer, W. E. *Phys. Rev. B* **1978**, *18*, 2792.

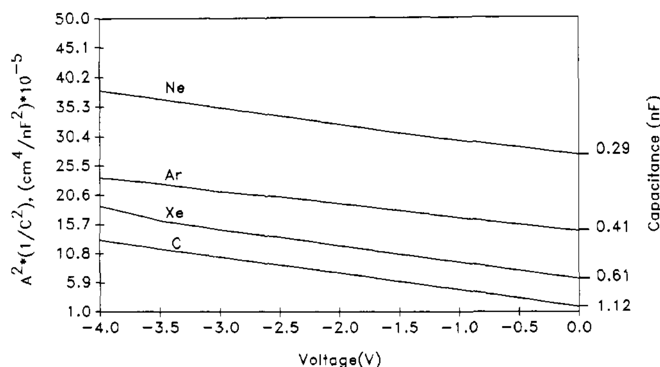

Figure 5. Capacitance–voltage characteristics for crystalline, 3-keV Xe^+-, Ar^+-, and Ne^+-ion-bombarded GaAs.

respond to second-order combination bands, such as 2LO. The LO and 2LO peaks are sensitive to disorder. Broadening of the LO peak and a decrease in its intensity indicate a disruption of the order and crystalline quality of the material. The LO peak intensity ratio for ion-bombarded GaAs to that for crystalline GaAs was evaluated. The intensity ratios for Xe^+-, Ne^+-, and $^3He^+$-ion-bombarded GaAs are 1.12, 0.83, and 0.79, respectively. A decrease in the intensity ratio and a broadening of the LO peak are observed for the ion-bombarded samples, reflecting bombardment-induced disorder. The broadening and decreased intensity of the LO peak are greatest for the lightest ion, $^3He^+$, showing that the lighter the ion, the deeper the damage.

From the trends observed in the reflectivity (Figure 3) and Raman spectra (Figure 4) for ion-bombarded GaAs, the effect on the damage depth caused by varying the mass of the bombarding ion can be assessed. It is evident from the reflectivity and Raman spectra that the lightest ion, $^3He^+$, causes structural damage that penetrates deep (>250 Å) into the GaAs crystal. With increasing mass of the bombarding ion, the depth of damage decreases with the heaviest ion, Xe^+, leaving behind a very shallow layer of damage (≈50 Å). Therefore, the damage depth is inversely related to the mass of the bombarding ion.

The current–voltage and capacitance–voltage results qualitatively support the optical results. Current–voltage measurements on each ion-bombarded diode revealed ion-induced current enhancement. The forward characteristics (ln current vs voltage) of such diodes were extremely nonlinear, the extent of nonlinearity being the least for the Xe^+-ion-bombarded diode. This indicated the likelihood of the creation of a thinner damaged layer resulting from Xe^+ than from Ar^+ or Ne^+ ion bombardment, at similar energy and fluence. The nonlinear forward characteristics for ion-bombarded diodes suggest the presence of additional processes, apart from thermionic emission, that contribute to current transport. Hence, diode parameters deduced for ion-bombarded diodes will, in all likelihood, be invalid. The control diode (nonbombarded GaAs), on the contrary, had current transport governed by thermionic emission, with ideality factor and reverse saturation current of 1.25×10^{-8} and 1.7×10^{-8} A, respectively.

The capacitance–voltage measurement results are shown in Figure 5. Although the electrical measurement probes much deeper (a few thousand angstroms) into GaAs than the structural damage extends, the damage layer will have a different capacitance than the crystalline substrate due to disruption in the crystal order. Thus one is essentially measuring two capacitors in series. Increasing the thickness of the damage layer would decrease the overall measured capacitance of the diode. The total measured

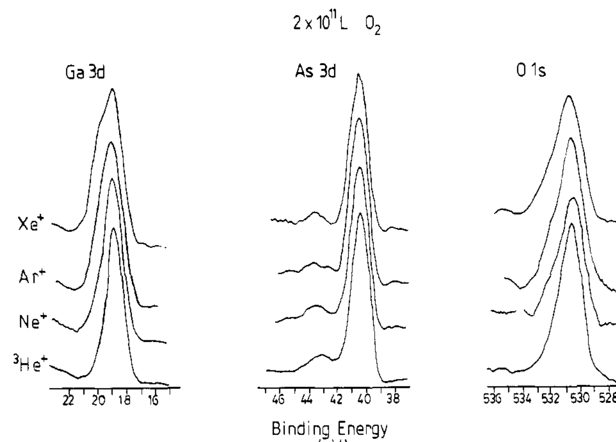

Figure 6. Representative spectra taken at 15° TOA for 3-keV $^3He^+$-, Ne^+-, Ar^+-, and Xe^+-ion-bombarded GaAs exposed to 2×10^{11} langmuirs of O_2.

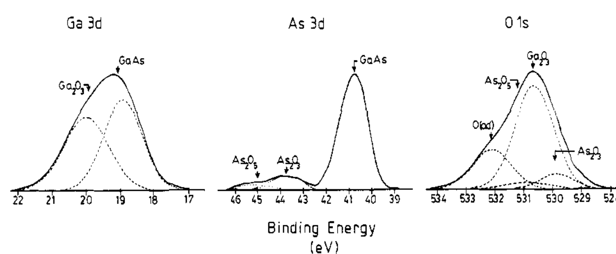

Figure 7. Representative curve-resolved spectra taken at a 15° TOA for 3-keV Xe^+-ion-bombarded GaAs exposed to 2×10^{11} langmuirs of O_2.

capacitance (see Figure 5) decreased after ion bombardment, with the greatest decrease occurring following bombardment with lighter mass ions. The decrease in capacitance implies that a damage layer is formed by ion bombardment and the depth of this layer is greater for lower mass ions. The capacitance was not measured for 3-keV $^3He^+$-ion-bombarded GaAs; however, from the trends indicated in the Raman and reflectivity spectra, it would be expected to show a lower capacitance than that for 3-keV Ne^+-ion-bombarded GaAs. The capacitance measured for 3-keV Xe^+ is closest to the value for crystalline material, indicating that the damage layer formed as a result of Xe^+-ion-bombardment was very thin. The effect of decreasing capacitance following ion bombardment has been reported previously in the literature.[15,21]

Effect of Bombarding Ion Mass on Reactivity. O_2 and H_2O Exposures. Chemically cleaned GaAs was ion bombarded with 3-keV $^3He^+$, Ne^+, Ar^+, and Xe^+ ions and subsequently exposed to 10^7, 10^8, and 2×10^{11} langmuirs of O_2. Representative XPS spectra obtained at a 15° TOA for each ion-bombarded GaAs following 2×10^{11} langmuirs of O_2 exposure are presented in Figure 6. The Ga 3d and As 3d photopeaks both exhibit evidence for the formation of oxides on the surface by the appearance of photopeaks on the high binding energy sides of the respective substrate photopeaks. The determination of chemical species in the photopeaks was accomplished by curve resolution. The curve resolution was carried out using Gaussian-type peaks. The peak positions and the fwhm's used in the curve resolution were determined by measuring XPS spectra for standard oxide compounds.[4] The fwhm and peak positions for the Ga 3d and As 3d due to GaAs were determined from the spectra for ion-bombarded GaAs. Oxygen peak intensities were selected on the basis of knowledge of the oxygen/gallium or oxygen/arsenic ratio for the respective gallium (Ga_2O_3) and arsenic (As_2O_3, As_2O_5) oxides.

Table III. Binding Energies for Surface Components

component	BE, eV	fwhm, eV
Ga(GaAs)	18.8 ± 0.1	1.2 ± 0.1
As(GaAs)	40.8 ± 0.1	1.5 ± 0.2
$Ga(Ga_2O_3)$	19.9 ± 0.2	1.4 ± 0.2
Ga(GaO(OH))	20.0 ± 0.2	1.5 ± 0.2
$Ga(Ga(OH)_3)$	20.8 ± 0.2	1.6 ± 0.2
$As(As_2O_3)$	43.8 ± 0.3	1.7 ± 0.1
$As(As_2O_5)$	44.9 ± 0.2	1.5 ± 0.2
$O(Ga_2O_3)$	530.6 ± 0.2	1.5 ± 0.2
$O(As_2O_3)$	530.0 ± 0.3	1.3 ± 0.1
$O(As_2O_5)$	530.5 ± 0.2	1.6 ± 0.2
O(GaO*(OH))	531.0 ± 0.2	1.7 ± 0.1
O(GaO(O*H))	532.0 ± 0.2	1.7 ± 0.1
$O(Ga(OH)_3)$	532.1 ± 0.2	1.9 ± 0.2
$O(O_{ads})$	532.1 ± 0.3	1.6 ± 0.2
$O(H_2O_{ads})$	533.1 ± 0.3	1.9 ± 0.2

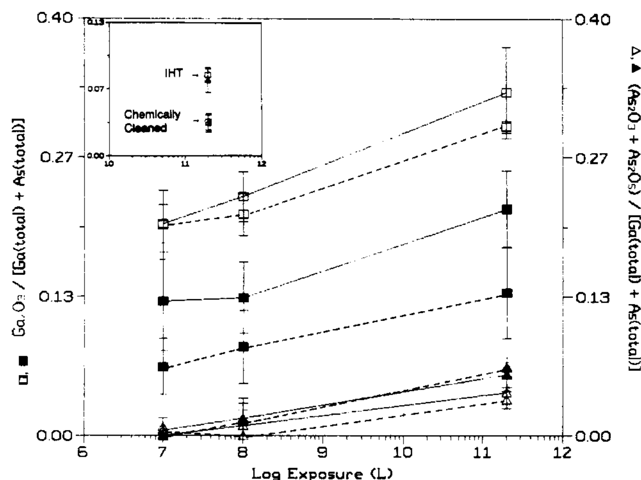

Figure 8. Relative amounts of gallium and arsenic oxides formed for 3-keV $^3He^+$ (--■--, --▲--), Ne^+ (-■-, -▲-), Ar^+ (--□--, --△--), and Xe^+ (-□-, -△-) ion-bombarded GaAs as a function of O_2 exposure. Squares (□, ■) represent gallium oxide, and triangles (△, ▲) represent arsenic oxide. Also included for reference (indicated in the expanded region inset at the top left) are those results for chemically cleaned and IHT-prepared GaAs exposed to 2×10^{11} langmuirs of O_2 obtained from the results of reference 4.

Typical curve-resolved spectra are shown in Figure 7 for 3-keV Xe^+-ion-bombarded GaAs exposed to 2×10^{11} langmuirs of O_2. These spectra are characterized by the photopeaks due to Ga(GaAs), As(GaAs), $Ga(Ga_2O_3)$, $As(As_2O_3, As_2O_5)$, $O(Ga_2O_3, As_2O_3, As_2O_5)$, and O(ad). Table III summarizes the binding energies obtained for the surface oxides on GaAs following O_2 exposure. The binding energies for surface oxides on GaAs compare favorably with the literature values tabulated in a previous publication.[4]

The relative quantities of gallium and arsenic oxides produced following O_2 exposure were determined from curve-resolved spectra and are shown in Figure 8 for the various ion-bombarded samples as a function of O_2 exposure and for chemically cleaned and IHT GaAs exposed to 2×10^{11} langmuirs of O_2.[4] The relative quantities of gallium or arsenic oxide are represented as

$$Ga(Ga_2O_3) \text{ or } [As(As_2O_3 + As_2O_5)]/[Ga(total) + As(total)] \quad (2)$$

Exposure of ion-bombarded GaAs to O_2 produces Ga_2O_3, As_2O_3, and As_2O_5 and adsorbed oxygen.[4] Preferential formation of Ga_2O_3 is noted. All of the ion-bombarded surfaces, regardless of the bombarding ion, produce approximately the same quantity of arsenic oxides, and this quantity is also the same as that found for chemically cleaned and IHT GaAs exposed to O_2.[4]

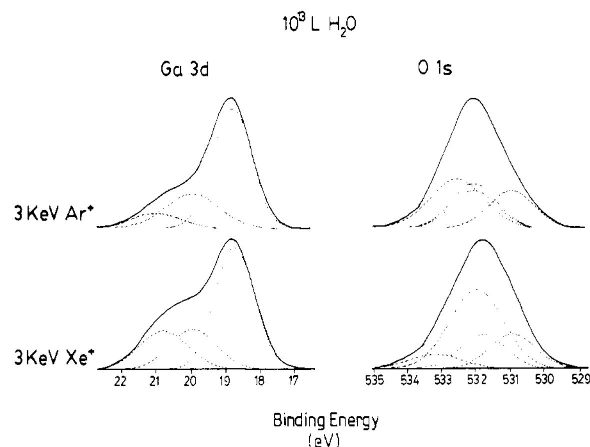

Figure 9. Curve-resolved XPS spectra taken at a 15° TOA for 3-keV Xe^+- and Ar^+-ion-bombarded GaAs exposed to 10^{13} langmuirs of H_2O.

The significant result is that the relative amount of Ga_2O_3 formed on ion-bombarded GaAs is greater for bombardment with heavier ions, with the amount of Ga_2O_3 formed being the greatest for the 3-keV Xe^+-ion-bombarded samples. This is most likely due to the greater number of defect sites in the surface layer produced by bombardment with the heavier ion. It was shown previously[4] that Ar^+-ion-bombardment had an effect on the chemical reactivity of GaAs, with Ga_2O_3 being the dominant species. The amount of Ga_2O_3 formed was shown not to be dependent on the Ga/As ratio by comparing the O_2 exposure results of Ar^+-ion-bombarded GaAs to those of IHT-prepared GaAs (see Figure 8). The previous result is reinforced here by examining the data for $^3He^+$-ion-bombarded GaAs exposed to O_2. The Ga/As atomic ratio for GaAs bombarded with $^3He^+$ ions was 1.16 ± 0.08 (15° TOA from Table I) and 1.23 ± 0.07 for IHT GaAs.[4] Comparing the relative amount of oxide produced following 2×10^{11} langmuirs of O_2 exposure for $^3He^+$ and IHT GaAs (see Figure 8), the average fraction of Ga_2O_3 formed upon O_2 exposure at 2×10^{11} langmuirs of O_2 is greater for $^3He^+$ than for IHT GaAs (0.13, 0.08, respectively), even though the Ga/As atomic ratios for the ion-bombarded but unexposed samples are almost the same. An important difference to note is not only the amount of Ga_2O_3 formed but the relative amounts of both gallium and arsenic oxides formed. IHT-prepared GaAs exhibited equal formation of both gallium and arsenic oxides, whereas the $^3He^+$ ion-bombarded GaAs exhibited the usual behavior of ion-bombarded material exposed to O_2; preferential formation of Ga_2O_3. Thus, it is apparent that the Ga/As ratio does not control the amount of oxide formed but that reactions are controlled by the number of defect sites that are formed by ion bombardment.

The curve-resolved Ga 3d and O 1s photopeaks (15° TOA) for 3-keV Xe^+ and Ar^+ ion-bombarded GaAs exposed to 10^{13} langmuirs of H_2O are shown in Figure 9. After H_2O exposure, a broadening occurs on the higher binding energy side of the Ga 3d photopeak while no change is observed for the As 3d photopeak. The adsorption and reaction of H_2O on ion-bombarded GaAs produces GaO(OH), $Ga(OH)_3$, and adsorbed H_2O.[4] Below 10^{10} langmuirs, GaO(OH) was determined to be the species present because the Ga 3d peak shifted to higher binding energy was broader than that expected for Ga_2O_3, and the presence of GaO(OH) was also supported by the shape of the O 1s photopeak. For H_2O exposures above 10^{10} langmuirs, the shape of the higher binding energy Ga 3d

Table IV. Data for 3-keV Xe^+- and Ar^+-Ion-Bombarded GaAs Exposed to 10^{13} Langmuirs of H_2O

ion	total oxide[a]	$Ga(OH)_3$[b]	$GaO(OH)$[b]	O-(H_2O_{ads}), at. %	O(total), at. %
Xe^+	0.340	0.172	0.168	4 ± 2	46 ± 5
Ar^+	0.228	0.064	0.164	14 ± 5	43 ± 5

[a] $[Ga(OH)_3 + GaO(OH)]/[Ga(total) + As(total)]$, ±10%. [b] $Ga(OH)_3$ or $GaO(OH)/[Ga(total) + As(total)]$, ±10%.

photopeak did not grow in intensity as would be expected if only Ga_2O_3 or GaO(OH) were present on the surface. Instead, the peak broadened more to the higher binding energy side indicating the presence of a new photopeak shifted 0.7–1.0 eV higher than that for GaO(OH). This new photopeak was attributed to the formation of another gallium-containing species, $Ga(OH)_3$. Thus, the spectra shown in Figure 9 are characterized by Ga(GaAs), Ga(GaO(OH)), Ga(Ga(OH)$_3$), O(GaO*(OH)), O(GaO(O*H)), O(Ga(OH)$_3$), and O(H_2O_{ads}). The binding energies obtained for these species are listed in Table III. The relative amounts of oxidized gallium species (GaO(OH) and Ga(OH)$_3$) produced following H_2O exposure are presented in Table IV along with the atomic percent of H_2O(ads) and total oxygen content.

The total amount of oxygen for 3-keV Xe^+ ion-bombarded GaAs exposed to 10^{13} langmuirs of H_2O is the same as that for 3-keV Ar^+ ion-bombarded GaAs exposed to 10^{13} langmuirs of H_2O, which suggests that each sample adsorbs an equivalent amount of H_2O. However, the total quantity of oxidized gallium is greater for the Xe^+-ion-bombarded sample, and the distribution of species is different (see Table IV). The relative amount of GaO(OH) is approximately the same for the two samples; however, the amount of $Ga(OH)_3$ is greater for the Xe^+-ion-bombarded sample. This finding indicates that the different ion-bombardment conditions and thus the presence of different amounts of surface damage have an effect on the dissociation of an adsorbed H_2O layer, with Xe^+-ion bombardment having the greatest effect on the reactivity.

The ion-bombardment process is influenced by the sputter yield, by the penetration range of the ions into the solid, and by the amount of energy and momentum initially transferred to the surface atoms that initiate the collision cascade. Damage in the crystal is affected by the mass, energy, and momentum of the bombarding ion. At a given ion energy, the range of damage increases with decreasing ion mass, while the amount of damage increases with increasing ion mass.

Optical, electrical, and surface characterization measurements[31] show that near-surface structural damage accompanies ion bombardment. In the present study, results for GaAs bombarded with different ions and exposed to O_2 or H_2O demonstrate that surface defects play a role in chemical reactivity. Enhanced reactivity was observed on ion-bombarded GaAs, and the enhancement increased with increasing ion mass. That the product distribution is not the same following bombardment with the different ions suggests that the reactivity is related to surface defect concentration and that the defect concentration is determined by the mass of the bombarding ion. It has been shown in this study that the depth of the bombardment-induced damage layer in GaAs is greater for lighter ions. On the basis of the chemical reactivity results, bombardment with heavier ions produces a greater defect concentration at the surface. The XPS data indicated that As was preferentially sputtered from at least the first 60 Å of the surface. Figure 10 illustrates a model for the removal of As during ion bombardment from GaAs surface

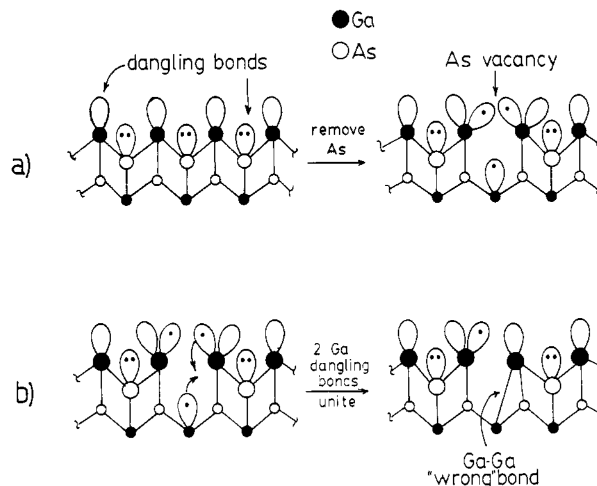

Figure 10. Schematic representation of (a) the removal of As from GaAs during ion bombardment to create As vacancies and singly occupied Ga dangling bonds and (b) two singly occupied Ga dangling bonds uniting to form Ga–Ga "wrong" bonds that could be possible defects that serve as sites for reactions on the ion-bombarded surface. The ion-bombarded surface is most likely more disordered than the structures indicated in this figure.

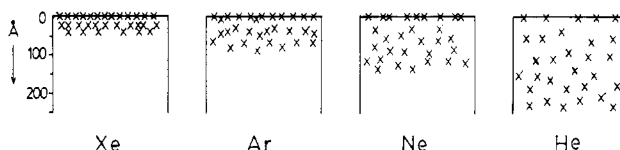

Figure 11. Schematic representation of the distribution of damage caused by ion bombardment with different mass ions.

and presents some possible postbombardment surface configurations, which are represented as As deficiencies, singly occupied Ga dangling bonds, and Ga–Ga "wrong" bonds.

A clear distinction should be made between the total *depth* and the near-surface *density* of the bombardment-induced structural damage. Since Raman scattering and UV reflectivity are sensitive to damage whose depth is an appreciable fraction of the optical penetration depth, these optical measurements have shown that the depth of damage decreases with increasing ion mass. The electrical capacitance measurements also reveal the same trend. On the other hand, the chemical reactivity studies are sensitive to the density of damage defects at, or very close to, the surface. The reactivity measurements show that the surface damage density increases with increasing ion mass. Defects are concentrated very close to the surface for bombardment with massive ions. These findings are qualitatively expressed in Figure 11.

Figure 11 schematically indicates the distribution of defects (defect sites) caused by bombardment with ions of different mass. Since the ion bombardments in this study were carried out at constant fluence, an equivalent number of chemically reactive defects (represented by crosses in Figure 11) is shown for each case; however, the distribution of these defects through the crystal is different depending on the mass of the bombarding ion. Xenon-ion bombardment causes a shallow damage layer confined close to the surface (approximately 50 Å deep), therefore imparting more defects at the surface—more broken Ga–As bonds, more As deficiencies, and more singly occupied dangling bonds. The defects caused by $^3He^+$ are more widely spread throughout the lattice to depths greater than 100 Å, and there are fewer defects at the surface. It has been suggested that initial oxidation occurs at surface

defect sites,[1,2,6,7,11,27,28,34-39] and since Xe^+-ion bombardment produces a greater concentration of defects at the surface, Xe^+-ion-bombarded GaAs exhibits a greater enhancement of surface oxidation. Lighter ions impart defects deep into the crystal, and therefore the concentration of defects (sites for reactions) at the surface is smaller and there is less enhancement in the reactivity. Also, any damage present far from the surface (the first few atomic layers) may be of a different form. Defects on the surface may be composed mainly of broken Ga–As bonds with many singly occupied Ga dangling bonds (see Figure 10), while deeper defects may have a chance to re-form bonds within the bulk and thus form unreactive centers.

Conclusions

The effect of bombarding ion mass on the chemical reactivity of GaAs was investigated for 3-keV $^3He^+$, Ne^+, Ar^+, and Xe^+ ions (constant fluence). Exposure of ion-bombarded GaAs surfaces to 10^7–10^{11} langmuirs of O_2 produced Ga_2O_3, As_2O_3, and As_2O_5 with the preferential formation of Ga_2O_3, and exposure to 10^{13} langmuirs of H_2O yielded both GaO(OH) and $Ga(OH)_3$. The greatest amount of oxidized gallium was found following exposure of 3-keV Xe^+-ion-bombarded GaAs to O_2 or H_2O. Comparison of the relative quantities of oxidized gallium formed on ion-bombarded GaAs to that formed on chemically cleaned or IHT-prepared GaAs supports the conclusion that reactions take place at defect sites that are formed by ion bombardment. Since the greatest reactivity was observed for Xe^+-ion-bombarded GaAs, this suggests that the greatest concentration of defects was present on a surface bombarded with Xe^+.

The damage caused by ion bombardment was investigated by optical reflectivity in the visible and near-ultraviolet region (1.6–5.6 eV), by Raman spectroscopy, and by current–voltage and capacitance–voltage measurements. Ion bombardment was shown to form a structurally damaged layer as evidenced by the destruction of the peaks due to crystalline GaAs in the optical reflectivity and Raman spectra, and from these spectra it could be determined that the depth of ion-bombardment damage was inversely related to the mass of the bombarding ion. A similar depth versus mass relationship was indicated by the capacitance–voltage measurements. The overall capacitance of ion-bombarded GaAs decreased as a function of decreasing ion mass. However, all of the ion bombardments resulted in measurable changes in diode electrical parameters, with the severity of the change decreasing with increasing ion mass. The findings of this study suggest possible ways to modify the surface of GaAs, with smaller damage depths occurring for bombardment with ions of heavier mass.

Acknowledgment. We acknowledge the funding of this project by Texas Instruments, the Virginia Center for Innovative Technology, and the National Science Foundation (via an equipment grant). We also thank Frank Cromer for his help with the surface analysis equipment.

Registry No. GaAs, 1303-00-0; $^3He^+$, 15644-29-8; Ne^+, 14782-23-1; Ar^+, 14791-69-6; Xe^+, 24203-25-6; H_2O, 7732-18-5.

(34) Barton, J. J.; Goddard III, W. A.; McGill, T. C. *J. Vac. Sci. Technol.* **1979**, *16*, 1178.
(35) Spicer, W. E.; Chye, P. W.; Garner, C.; Lindau, I.; Pianetta, P. *Surf. Sci.* **1979**, *86*, 763.
(36) Ranke, W.; Jacobi, K. *Surf. Sci.* **1979**, *81*, 504.
(37) Bartels, F.; Mönch, W. *Surf. Sci.* **1984**, *143*, 31.
(38) Bartels, F.; Surkamp, L.; Clemens, H. J.; Mönch, W. *J. Vac. Sci. Technol. B* **1983**, *1*, 756.
(39) Mark, P.; Chang, C.; Creighton, W. F.; Lee, B. W. *CRC Crit. Rev. Solid State Mater. Sci.* **1975**, *5*, 189.

Aromatic Hydrocarbon Intercalates: Synthesis and Characterization of Iron Oxychloride Intercalated with Perylene and Tetracene

Joseph F. Bringley† and Bruce A. Averill*

Department of Chemistry, University of Virginia, Charlottesville, Virginia 22901

Received October 12, 1989

The reaction of a series of polycyclic aromatic hydrocarbons with the layered host FeOCl has been examined. Arenes with ionization potentials ≤ca. 7 eV react with FeOCl via an intercalation process. The intercalation compounds $FeOCl(perylene)_{1/9}$ and $FeOCl(tetracene)_{1/12}$ have been characterized. Powder X-ray diffraction studies of microcrystalline powders and oriented films of these materials indicate that in each case the guest molecules are oriented with their molecular planes perpendicular to the layers of the host lattice. FTIR spectra indicate that intercalation of these molecules into FeOCl occurs via a redox mechanism, in which approximately one electron is transferred to the host lattice per guest molecule. Temperature dependent conductivity measurements show a 10^5-fold increase in conductivity over that of unintercalated FeOCl, with apparent bandgaps of 0.29 and 0.27 eV for the perylene and tetracene intercalates, respectively.

Introduction

The lamellar transition-metal oxyhalides (MOX: M = Ti, V, Cr, X = Cl, Br; M = Fe, X = Cl) are able to undergo intercalation reactions that involve the reversible insertion of guest species (i.e., atoms or molecules) between infinite two-dimensional sheets of the host. The host layers expand to accommodate the preferred orientation of the guest, as interlayer host–host interactions are replaced by more favorable host–guest and guest–guest interactions. Only relatively minor changes in the host structure accompany the intercalation process.[1-4] Among the layered

† Present address: IBM Research Division, Thomas J. Watson Research Center, Yorktown Heights, NY 10598.
* To whom correspondence should be addressed.

(1) Halbert, T. R. In *Intercalation Chemistry*; Whittingham, M. S., Jacobson, A. J., Eds.; Academic Press: New York, 1982; Chapter 12.

0897-4756/90/2802-0180$02.50/0 © 1990 American Chemical Society